

## APPLICATION OF POSITRON ANNIHILATION SPECTROSCOPY FOR CHARACTERIZATION AND MICROSTRUCTURAL STUDIES OF ULTRA-FINE GRAINED CUBIC METALS \*

Ivan PROCHÁZKA <sup>a</sup>, Jakub ČÍŽEK <sup>a</sup>, Radomír KUŽEL <sup>a</sup>, Zdeněk MATĚJ <sup>a</sup>, Miroslav CIESLAR <sup>a</sup>,  
Gerhard BRAUER <sup>b</sup>, Wolfgang ANWAND <sup>b</sup>, Rinat K. ISLAMGALIEV <sup>c</sup>

<sup>a</sup> *Department of Low Temperature Physics, Faculty of Mathematics and Physics, Charles University in Prague, V Holešovičkách 2, CZ-180 00 Praha 8, Czech Republic,  
E-mail address ivan.prochazka@mff.cuni.cz*

<sup>b</sup> *Institute of Radiation Physics, Forschungszentrum Dresden-Rossendorf, P.O. Box 510119,  
01314 Dresden, Germany*

<sup>c</sup> *Institute of Advanced Materials, Ufa State Aviation Technical University, ul. K. Marksa 12, Ufa,  
450000 Bashkortostan, Russia*

### Abstract

Present Contribution is focused on investigations of bulk ultra-fine grained (UFG) cubic metals (Cu, Ni, Fe), prepared by severe plastic deformation (high-pressure torsion). Recent results obtained within Prague – Dresden – Ufa collaboration are reviewed. Positron annihilation spectroscopy (PAS) was employed as the main experimental technique in these studies, including conventional PAS as well as positron beam measurements. Defects, induced by deformation, were identified, their lateral and depth distributions were studied. The influence of preparation conditions and ceramic Al<sub>2</sub>O<sub>3</sub> nanoparticles on thermal stability of UFG copper was examined.

### 1. INTRODUCTION

During the last three decades, it has been well-established that grain refinement of the ordinary polycrystalline metals far below 1 μm can lead to a remarkable improvement of their mechanical, electrical and thermal properties. Materials characterized by an average grain size of few hundreds of nanometers are classified as ultra-fine grained (UFG) ones. Among the techniques of UFG materials production, those based on the severe plastic deformation (SPD) are the most promising since they are capable to provide macroscopic amounts of material with negligible residual porosity [1]. SPD processing, however, results in a highly non-equilibrium state of the material with a huge amount of various kinds of deformation-induced microstructural defects, especially vacancies, dislocations, vacancy agglomerates and defects related to grain boundaries (GB's). These defects, in turn, can substantially influence the formation and stability of UFG structure and, consequently, macroscopic properties and practical use of the material. Obviously, structural studies of the SPD-made UFG materials on an atomic arrangement scale are of a key importance, since they assist to understanding the mechanism of the UFG structure formation and behaviour (especially its thermal stability). Moreover, such investigations serve as a guide how to optimize production processes.

Positron annihilation spectroscopy (PAS) is a well-recognized experimental method of investigation of small-size open-volume defects. In particular, defect type and concentration can be determined with a high

---

\* This work was supported by The Grant Agency of the Academy of Sciences of the Czech Republic within the scientific program "Nanotechnology for Society" (project KAN 300100801) and by the Ministry of Education, Youth and Sports of the Czech Republic (scientific plan MSM 2062081134).

sensitivity [2]. Moreover, typical positron diffusion lengths in metals are comparable with the average grain size of UFG materials. Hence, positrons can also effectively probe GB's. Therefore, PAS is an efficient tool of microstructural studies of UFG materials.

In the present Contribution, a review of recent investigations on UFG cubic metals Cu, Fe, Ni is presented. These investigations were conducted within Prague – Dresden – Ufa collaboration and involved materials prepared by high-pressure torsion (HPT). PAS was used as the principal experimental technique of probing materials studied: (i) the conventional PAS employing directly positrons from  $^{22}\text{Na}$ , and (ii) the slow-positron implantation spectroscopy (SPIS) utilizing a monoenergetic beam of slow positrons. PAS investigations were combined with transmission electron microscopy (TEM) observations, X-ray diffraction (XRD) and microhardness measurements. First, we will focus on characterization of as-deformed cubic metals with UFG structure. The formation of UFG structure and its thermal stability during isochronal annealing will be discussed. Finally, the role of metal oxide nanoparticles on thermal stability of UFG structure will be illustrated on an example of alumina ( $\text{Al}_2\text{O}_3$ ) nanoparticles embedded in UFG Cu.

## 2. EXPERIMENTS

### 2.1. Samples

The high-purity (>99.95 %) Cu, Fe Ni metals and commercial  $\text{Cu}+\text{Al}_2\text{O}_3$  GlidCop™ nanocomposites (SCM Metal Products) with three different contents,  $x$ , of  $\text{Al}_2\text{O}_3$  ( $x = 0.3, 0.5$  and  $1.1$  wt.%) were HPT-processed at room temperature (RT) using a technique described in Ref. [1]. Torsion was applied up to a true logarithmic strain of  $\epsilon = 7$  under a high uniaxial pressure of  $P = 6$  GPa. To elucidate a possible role of pressure, UFG Cu specimens HPT-deformed under  $P = 3$  GPa were also prepared. The specimens were disk-shaped with a diameter of 10 to 12 mm and a thickness of 0.2 to 0.4 mm.

### 2.2. Measurements and data analysis

*Conventional PAS.* In conventional PAS, positrons emitted by a proper radioisotope source are directly implanted into the material studied. Since such energetic positrons, ranging typically over an interval of several hundreds of keV, penetrate to depths of  $\approx 0.1$  mm in metals, depth profiling of microstructure on a micrometer scale is practically impossible in such a case. In our investigations, a carrier free  $^{22}\text{Na}$  in chloride or carbonate solution (Amersham, iThemba Labs) was utilized as a positron source. A drop of the  $^{22}\text{Na}$  in solution, containing  $\approx 1.5$  MBq activity, was dried and sealed between 2  $\mu\text{m}$  mylar D foils (DuPont). The diameter of the radioactive spot was  $\approx 3$  mm. The source was sandwiched between two identical pieces of material studied.

Conventional positron lifetime (PL) measurements were performed using a  $\text{BaF}_2$  lifetime spectrometer described in Ref. [3]. The spectrometer exhibited a time resolution of 150 to 170 ps (FWHM) for  $^{22}\text{Na}$  and a coincidence count rate of  $\approx 100$  s $^{-1}$ . At least  $10^7$  counts were collected in each PL spectrum. Decomposition of measured spectra into up to 5 exponential components was performed using a maximum-likelihood procedure [3]. The two of these components were always attributed to  $\approx 7$  % contribution arising from positron annihilations in the source.

Conventional Doppler broadening (DB) measurements were carried out using a standard HPGe  $\gamma$ -spectrometer showing an energy resolution of 1.2 keV (FWHM) at 511 keV energy. At least  $10^6$  counts were

collected in each annihilation line. The shape of the line was characterized in terms of ordinary sharpness ( $S$ ) and wing ( $W$ ) parameters. The  $S$ -parameter is the relative contribution of the central part to the total area of the annihilation line, while the  $W$ -parameter is relative contribution of the annihilation line tails. Thus the  $S$ -parameter expresses a contribution from low-momentum electrons and its greater value may indicate an increased role of positron trapping in open-volume defects. On the other hand, the  $W$ -parameter is a response to high-momentum electrons from inner shells of atoms surrounding the positron annihilation site.

*SPIS.* Contrary to the conventional PAS, the SPIS technique allows for depth profiling of microstructure on a micrometer scale. SPIS experiments of the present work were carried out using the magnetically guided positron beam facility "SPONSOR" at FZ Dresden-Rossendorf [4]. The beam diameter at the sample surface was  $\approx 4$  mm. Line shapes of annihilation  $\gamma$ -rays were measured using a HPGe spectrometer having an energy resolution of of 1.09 keV (FWHM) at 511 keV energy. Dependences of annihilation line shape parameters ( $S$  and  $W$ ) on positron energy were investigated in the interval 30 eV to 35 keV and analyzed by means of the VEPFIT code [5].

*Other techniques.* TEM observations were carried out using a JEOL 2000 FX electron microscope operated at 2000 kV. XRD measurements were performed by means of a XRD7 and HZG4 powder diffractometers (Seifert-FPM). The Cu  $K_{\alpha}$  radiation was employed in the XRD experiments. Microhardness  $HV$  was measured by means of the Vickers method using a LECO M-400-A hardness tester with a load of 100 g applied for 10 s.

### 3. RESULTS AND DISCUSSION

The results received in our recent investigations of HPT-deformed UFG Cu, Ni, Fe metals and Cu+Al<sub>2</sub>O<sub>3</sub> nanocomposites [6-12] are overviewed in this section.

#### 3.1. Microstructure of as-deformed specimens

As-deformed UFG materials were first characterized by means of conventional PL spectroscopy and the results of these measurements are summarized in Table 1. In all the measured UFG metals, two lifetime components (lifetimes  $\tau_i$  and relative intensities  $I_i$ ,  $i=2,3$ ) could be resolved. The lifetimes  $\tau_i$  of Tab. 1 significantly exceed the single-component values  $\tau_{\text{bulk}}$  found in respective well-annealed metals, 114 ps in Cu [6], 110 ps in Ni [8] and 108 ps in Fe [3]. This is a strong evidence that all positrons in UFG metals of Tab. 1 annihilate from trapped states at defects indicating simultaneously a high defect densities created by SPD. The dominating lifetime components ( $\tau_2$ ,  $I_2$ ) exhibit by about 10 ps shorter lifetimes than those observed for positrons trapped in monovacancies in respective metals: 168 – 170 ps in Cu, Ni [13], 180 ps in Fe [14]. Such a behaviour is characteristic for positrons trapped at dislocations [2]. TEM observation of microstructure of HPT-made UFG Cu, Ni and Fe were also involved in the present studies. These observations revealed a highly fragmented microstructure with a mean grain size of  $\approx 110 \div 150$  nm and mostly high-angle type GB's. Moreover, a high dislocation density is indicated by TEM with a strongly non-uniform spatial distribution of dislocations inside grains: grain interiors almost free of dislocations are surrounded by distorted regions with a high dislocation density, situated along GB's. Therefore, one can conclude that the  $\tau_2$ -components of Tab. 2 originate from positrons trapped at dislocations in the distorted regions along GB's. However, such a non-uniform spatial distributions of dislocations inside grains cannot be

regarded as a general feature of HPT. It is obviously inherent to the cubic metals and not to the hcp structures, as dislocations in HPT-processed UFG Mg alloys were found to be distributed homogeneously [15].

**Table 1**

Positron lifetimes  $\tau_i$  and relative intensities  $I_i$  ( $i = 2,3$ ) observed in as-deformed UFG materials. Errors (the 1 standard deviation) are given in parentheses in units of the last significant digit. Number of vacancies,  $n_V$ , in a vacancy cluster equivalent in size to observed microvoids is also shown – see the text for further details.

Sample	$\tau_2$ [ps]	$I_2$ [%]	$\tau_3$ [ps]	$I_3$ [%]	$n_V$
Cu, HPT (6 GPa)	161(3)	64(4)	249(5)	36(4)	4.8(3)
Cu, HPT (3 GPa)	164(1)	83(4)	255(4)	17(3)	5.2(3)
Cu+Al <sub>2</sub> O <sub>3</sub> (x=0.3 wt.%), HPT (6 GPa)	166(1)	80(1)	295(5)	20(1)	7.4(4)
Cu+Al <sub>2</sub> O <sub>3</sub> (x=0.5 wt.%), HPT (6 GPa)	165(2)	71(1)	301(4)	29(1)	7.9(3)
Cu+Al <sub>2</sub> O <sub>3</sub> (x=1.1 wt.%), HPT (6 GPa)	166(1)	70(1)	297(3)	30(1)	7.4(3)
Ni, HPT (6 GPa)	157(1)	88.9(6)	336(8)	11.1(6)	13.1(6)
Fe, HPT (6 GPa)	150.9(4)	90.6(3)	352(6)	9.5(3)	13.2(5)

The  $\tau_3$ -components exhibit lifetimes above 240 ps and represent obviously a contribution of positrons trapped in microvoids of a size equivalent to a few-vacancy cluster. The number of vacancies,  $n_V$ , constituting such clusters could be estimated from comparison of the observed  $\tau_3$ -values with those calculated for the clusters of various size within the density functional theory. Details of these calculations were presented elsewhere [6,8,16] and resulting  $n_V$ -values were shown in the last column of Tab. 1. A formation of vacancy clusters seems to be substantiated here since a large number of vacancies are created during SPD. These vacancies are mobile at RT [17] and thus they are likely to form small vacancy clusters in dislocation-free grain interiors. Microvoids in Cu+Al<sub>2</sub>O<sub>3</sub> nanocomposites are slightly larger (7 to 8 vacancies) than in pure copper (4 to 5 vacancies). The cluster formation appears to be suppressed in HPT-deformed Mg-Gd alloys with hcp structure and homogeneous distribution of dislocations acting as an obstacle of vacancy movement [15]. The data of Tab. 1 suggest that the size of microvoids is driven by the material, probably due to different vacancy mobilities in different metals, and an influence of the deformation technique is of less importance.

### 3.2. Spatial distribution of defects in UFG pure copper and Cu+0.5wt.%Al<sub>2</sub>O<sub>3</sub> nanocomposite

Since the torsion deformation-induced strains increase from the centre to the edge of specimen, inhomogeneous spatial distribution of defects in HPT-made UFG specimens can be expected. The spatial distribution of defects was investigated using an UFG pure Cu and Cu+Al<sub>2</sub>O<sub>3</sub> nanocomposite (x = 0.5 wt.%) specimens, HPT-deformed under 6 GPa. SPIS as well as conventional PL and DB experiments were carried out and supplemented by TEM, XRD and microhardness measurements [7,12]. In order to enlarge the depth scale, probed in SPIS measurements, the pure Cu specimen was subjected to a controlled removal of a

surface layer by chemical etching [7]. In Figure 1, measured  $S$ -parameters are plotted versus positron energy  $E_+$  for a set of different layers removed by etching. The  $S$ -values at  $E_+ > 20$  keV, which correspond to positron annihilation in the bulk, were found to decrease gradually up to an 18  $\mu\text{m}$  layer removed. It indicates a decrease in defect concentration towards the sample interior up to about 18  $\mu\text{m}$  depth. No further decrease in the bulk  $S$ -values was observed. At larger depths, consequently, defects concentration remains unchanged. Combining SPIS results with XRD investigations (see Ref. [7] for details) suggests that the observed decrease of the bulk  $S$ -values is essentially due to a decrease in concentration of microvoids and also a light increase in grain size with increasing depth.

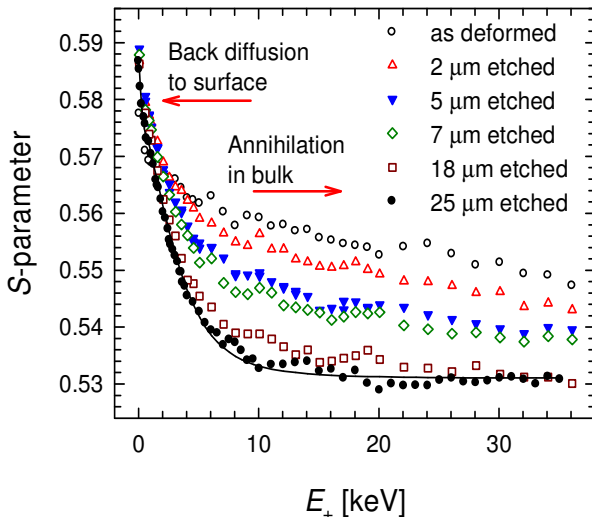


**Fig. 1.**  $S$ -parameters as functions of positron energy  $E_+$  for UFG Cu, HPT-deformed under 6 GPa. Data points: the measured values for the specimen subjected to a controlled chemical etching. Solid line: the VEPFIT fitted curve.

Radial changes in defect densities in UFG Cu were examined by means of SPIS, conventional PAS, TEM, XRD and microhardness measurements. Microhardness results clearly indicate a radial increase of defect density from the centre towards the edge of the sample [12]. The latter effect is illustrated in Fig. 2a. Moreover, PAS results revealed that the concentration ratio of microvoids to that of dislocations increases from the sample centre towards its margin [12].

### 3.3. Thermal stability of UFG pure copper

Thermal stability of UFG structure is an important property from the point of practical applications of UFG materials as well as for understanding physical processes underlying structure formation and stability. In our papers [6,10], isochronal annealing curves for HPT-made UFG pure Cu were studied. The two specimens deformed under 3 and 6 GPa were compared. The difference in deformation pressure is reflected by a difference in the mean grain size observed by TEM: 150 and 105 nm, respectively [10]. Each annealing step (30 °C / 30 min) was finished by quenching to water at RT. PL spectra were measured after each annealing step. PL data were analyzed in terms of the diffusion trapping model (DTM) developed and successfully applied to UFG Cu in Ref. [6]. Independently of applied pressure, the evolution of UFG structure proceeds through the two subsequent stages: (i) the abnormal grain growth when isolated recrystallized grains appear in essentially unchanged deformed matrix, and (ii) the recrystallization in the whole sample volume at higher temperatures. Activation energy of recrystallization, as deduced from annealing data on UFG Cu specimens, is in reasonable correspondence with the activation energy of migration of the equilibrium grains in the coarse-grained Cu [6]. The recrystallization onset was identified at around 300 and 190 °C, respectively, in the HPT-deformed Cu under 3 and 6 GPa. It indicates that finer grains lead to a lower thermal stability of UFG structure.

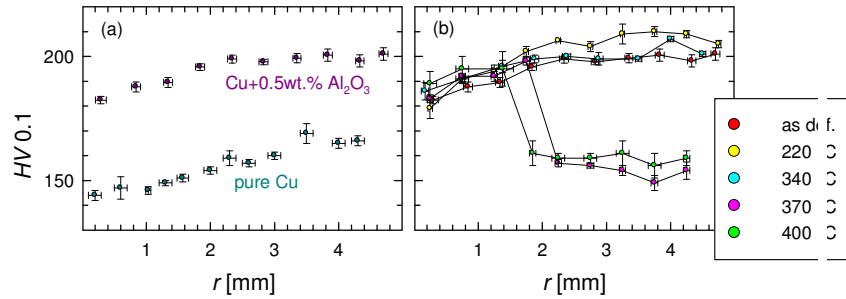


**Fig. 2.** The dependence of Vickers microhardness,  $HV$ , on radial distance,  $r$ , from sample axis: (a) a comparison of the as-deformed UFG pure Cu and Cu+0.5 wt.%  $Al_2O_3$ , (b) the evolution of microhardness during isochronal annealing of UFG Cu+0.5 wt.%  $Al_2O_3$  (annealing temperatures are shown in the insert).

### 3.4. Influence of alumina nanoparticles on thermal stability of UFG copper

An addition of ceramic particles is expected to be a promising way of improving thermal stability of UFG Cu. Ceramic particles are stable up to very high temperatures. If finely dispersed, ceramic particles act as efficient obstacles of dislocation and GB's movement, hindering thus grain growth. In this subsection, the

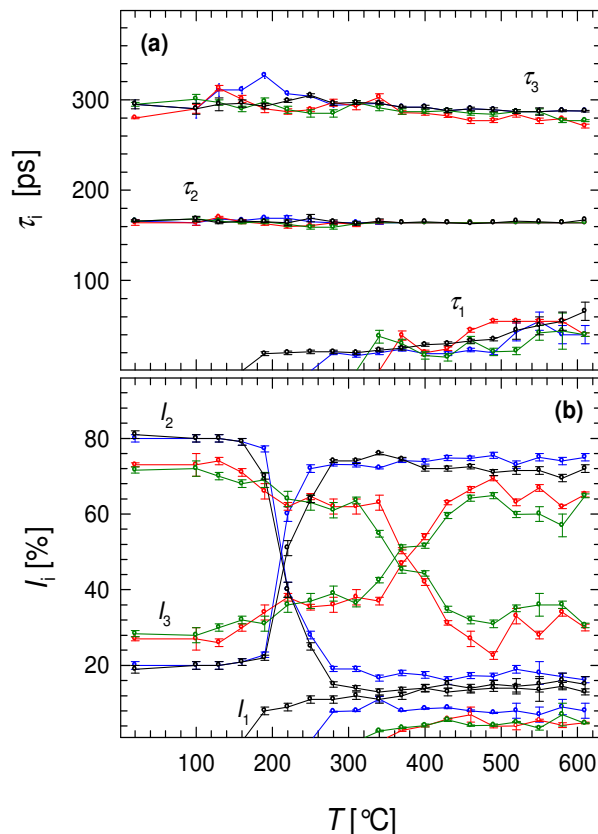


**Fig. 3.** The variations of PL parameters during isochronal annealing: a) positron lifetimes  $\tau_i$ , (b) relative intensities  $I_i$ ,  $i = 1, 2, 3$ ; — pure Cu, — 0.3 wt.%  $Al_2O_3$ , — 0.5 wt.%  $Al_2O_3$ , — 1.1 wt.%  $Al_2O_3$ .

results of our earlier investigations [7,12] on the HPT-made UFG Cu+ $Al_2O_3$  composite with different content of alumina nanoparticles are overviewed and compared with results obtained for pure UFG Cu. The aim of these investigations was to examine the effect of alumina nanoparticles and estimate their optimum content.

Annealing curves for Cu+ $Al_2O_3$  composites were measured by means of conventional PL technique and analyzed in a similar manner as described in the preceding subsection. The results are collected in Fig. 3. For a comparison, relative intensities  $I_i$  for the pure UFG copper were included, too. It can be seen from Fig. 3a, that lifetimes  $\tau_2$  and  $\tau_3$  were resolved in all nanocomposites and remain almost constant in the whole range of annealing temperatures. It is plausible to attribute the  $\tau_2$ - and  $\tau_3$ -components to positron trapping at dislocations and in microvoids, respectively. At higher annealing temperatures, a short lifetime components (lifetime  $\tau_1 < \tau_{bulk}$ ) starts to grow up. It clearly indicates the  $\tau_1$ -components as originated from annihilation of delocalized positrons. A sharp drop in intensity  $I_2$ , attributed to positrons trapped at dislocations along GB's, is observed at a certain temperature for each composite. It should be regarded

as an indication of recrystallization. The recrystallization onset temperatures of 190, 200, 340 and 340 °C can be read from Fig. 3b, for pure Cu,  $x = 0.3, 0.5$  and  $1.1$  wt.% composites, respectively. This allows to conclude that an optimum abundance of  $\text{Al}_2\text{O}_3$  nanoparticles providing a maximum thermal stability of  $\text{Cu}+\text{Al}_2\text{O}_3$  UFG structure amounts approximately 0.5 wt.% and an improvement of the recrystallization onset temperature by  $\approx 150$  °C may be attained.

An evidence of centripetal character of recrystallization in UFG  $\text{Cu}+0.5$  wt.%  $\text{Al}_2\text{O}_3$  was gained from a series of TEM images, taken for different annealing temperatures [12], and microhardness measurements,  $H_V$  [12]. The latter data are plotted in Fig. 2b as functions of radial distance from sample centre. A steep drop in  $H_V$  from values typical for a well developed UFG structure to those characteristic for the recrystallized one is observed for 370 and 400 °C annealing temperatures. The drop is shifted towards the sample centre for the higher annealing temperature. Such a behaviour may be understood as a consequence of a greater deformation energy stored at the margin compared to the centre of the specimen. Since the deformation energy is a driving force for the recovery of UFG structure, recrystallization begins at the edge and progresses towards the centre of the specimen.

#### 4. CONCLUDING REMARKS

The HPT-made bulk UFG pure cubic metals (Cu, Ni, Fe) and  $\text{Cu}+\text{Al}_2\text{O}_3$  nanocomposites with different content of alumina nanoparticles were systematically investigated by conventional PAS and SPIS, supplemented by TEM, XRD and microhardness measurements. The as-deformed specimens exhibited a highly fragmented structure with mainly high-angle GB's, a mean grain size of  $110 \div 150$  nm and a high dislocation density. A high average defect density with strongly inhomogeneous spatial distribution of dislocations over a grain was observed and seems to be characteristic for UFG cubic metals: dislocations are concentrated in the distorted regions along GB's, while grain interiors remain almost free of dislocations. Microvoids equivalent in size to clusters of  $4 \div 5$  vacancies in pure Cu,  $\approx 13$  vacancies in Ni, Fe and  $7 \div 8$  vacancies in  $\text{Cu}+\text{Al}_2\text{O}_3$  were observed. Moreover, depth and lateral variations of defect densities were detected.

The thermal stability of the HPT-made UFG structures in pure Cu and  $\text{Cu}+\text{Al}_2\text{O}_3$  nanocomposites were examined in isochronal annealing experiments. It was demonstrated that a higher deformation pressure leads to a smaller grain size but worsens thermal stability. An addition of alumina nanoparticles improves significantly thermal stability of UFG structure and an optimum amount of  $\text{Al}_2\text{O}_3$  nanoparticles lies around 0.5 wt.%.

#### LITERATURE REFERENCES

- [1] VALIJEV, R.Z., ISLAMGALIEV, R.K., ALEXANDROV, I.V. Bulk nanostructured materials from severe plastic deformation. *Progress in Materials Science*, 2000, Vol. 49, page 103.
- [2] HAUTOJÄRVI, P., CORBEL, C. Positron spectroscopy of defects in metals and semiconductors. In: *Positron spectroscopy of solids*. International School of Physics «Enrico Fermi», Course CXXV (ed. by DUPASQUIER, A. and MILLS, A.P., Jr.): Amsterdam, IOS Press, 1995, page 491.

- [3] BEČVÁŘ, F., et al. A high-resolution BaF<sub>2</sub> positron lifetime spectrometer and experience with its long-term exploitation. *Nuclear Instruments & Methods in Physics Research A*, 2000, Vol. 443, Iss. 2-3, page 557.
- [4] ANWAND, W., KISSENER, H.-R., BRAUER, G. A magnetically guided slow positron beam for defect studies. *Acta Physica Polonica A*, 1995, Vol. 88, Iss. 1, page 7.
- [5] VAN VEEN, A., et al. VEPFIT applied to depth profiling problems. *Applied Surface Sci.*, 1995, Vol. 85, Iss. 1, page 216.
- [6] ČÍŽEK, J., et al. Thermal stability of ultrafine grained copper. *Physical Review B*, 2002, Vol. 65, Iss. 9, article 094106.
- [7] ČÍŽEK, J., et al. Spatial distribution of defects in ultra-fine grained copper prepared by high pressure torsion. *Physica Status Solidi A*, 2003, Vol. 195, Iss. 2, page 335.
- [8] ČÍŽEK, J., et al. Positron lifetime investigation of thermal stability of ultra-fine grained nickel. *Physica Status Solidi A*, 2002, Vol. 191, Iss. 2, page 391.
- [9] ČÍŽEK, J., et al. Influence of Al<sub>2</sub>O<sub>3</sub> nanoparticles on the thermal stability of ultra-fine grained copper prepared by high pressure torsion. *Monatshefte für Chemie*, 2002, Vol. 133, Iss. 6, page 873.
- [10] ČÍŽEK, J., et al. Dependence of thermal stability on ultra fine grained metals on grain size. From Conference Proceedings *Nanomaterials by severe plastic deformation – NANOSPD2*. Weinheim: 2004, Wiley-VCH Verlag GmbH&Co. KGaA, page 630.
- [11] ČÍŽEK, J., et al., Ultra fine-grained metals prepared by severe plastic deformation: a positron annihilation study. *Acta Physica Polonica A*, 2005, Vol. 107, 2005, Iss. 5, page 738.
- [12] ČÍŽEK, J. et al. Influence of ceramic nanoparticles on thermal stability of ultra fine grained copper. *Acta Physica Polonica A*, 2008, Iss. 5, page 1285.
- [13] STAAB, T.E.M., KRAUSE-REHBERG, R., KIEBACK, J. Positron annihilation in finegrained materials and fine powders – an application to the sintering of metal powders. *Journ. of Materials Sci.*, 1999, Vol. 34, Iss. 16, page 3833.
- [14] SEEGER A., BANHART, F. On the systematics of positron lifetimes in metals. *Physica Status Solidi A*, 1987, Vol. 102, Iss. 1, page 171.
- [15] ČÍŽEK, J., et al. Microstructure and thermal stability of ultra fine grained Mg and Mg-Gd alloys prepared by high-pressure torsion. *Materials Sci. Forum*, 2005, Vol. 482, Iss. 1, page 183.
- [16] HEMPEL, A., et al. Effects of neutron irradiation on Fe-Cu model alloys and RPV steels probed by positron annihilation and hardness measurements. From Conference Proceedings: *Effects of Radiation on Materials, 19th Internat. Symp. ASTM STP 1366* (editors SMITH, A.B., JONES, C.D.). West Conshohocken: 1998, American Society for Testing Materials, page 560.
- [17] VAN DEN BEUKEL., A. From Conference Proceedings: *Proc. Int. Conf on Vacancies and Interstitials in Metals* (editors SEEGER, A., SCHUMACHER, D., SCHILLING, W., DIEHL, J.). Amsterdam: 1970, North-Holland, page 427.